CARDIORESPIRATORY DISEASE

Visualization of exhaled breath metabolites reveals distinct diagnostic signatures for acute cardiorespiratory breathlessness

Wadah Ibrahim[1]†, Michael J. Wilde[2,3]*†, Rebecca L. Cordell[2]†, Matthew Richardson[1], Dahlia Salman[4], Robert C. Free[1], Bo Zhao[5,6], Amisha Singapuri[1], Beverley Hargadon[1], Erol A. Gaillard[1], Toru Suzuki[7,8], Leong L. Ng[7], Tim Coats[9], Paul Thomas[4], Paul S. Monks[2], Christopher E. Brightling[1], Neil J. Greening[1], Salman Siddiqui[1,10]*, On behalf of the EMBER Consortium

Acute cardiorespiratory breathlessness accounts for one in eight of all emergency hospitalizations. Early, noninvasive diagnostic testing is a clinical priority that allows rapid triage and treatment. Here, we sought to find and replicate diagnostic breath volatile organic compound (VOC) biomarkers of acute cardiorespiratory disease and understand breath metabolite network enrichment in acute disease, with a view to gaining mechanistic insight of breath biochemical derangements. We collected and analyzed exhaled breath samples from 277 participants presenting acute cardiorespiratory exacerbations and aged-matched healthy volunteers. Topological data analysis phenotypes differentiated acute disease from health and acute cardiorespiratory exacerbation subtypes (acute heart failure, acute asthma, acute chronic obstructive pulmonary disease, and community-acquired pneumonia). A multibiomarker score (101 breath biomarkers) demonstrated good diagnostic sensitivity and specificity (≥80%) in both discovery and replication sets and was associated with all-cause mortality at 2 years. In addition, VOC biomarker scores differentiated metabolic subgroups of cardiorespiratory exacerbation. Louvain clustering of VOCs coupled with metabolite enrichment and similarity assessment revealed highly specific enrichment patterns in all acute disease subgroups, for example, selective enrichment of correlated C5-7 hydrocarbons and C3-5 carbonyls in heart failure and selective depletion of correlated aldehydes in acute asthma. This study identified breath VOCs that differentiate acute cardiorespiratory exacerbations and associated subtypes and metabolic clusters of disease-associated VOCs.

INTRODUCTION

Breathlessness due to cardiorespiratory diseases accounts for more than one in eight of all emergency admissions to hospital (*1*). Despite the same presenting symptom, the etiology of acute breathlessness is highly varied, with diverse disease trajectories and therapeutic options. Diagnostic evaluation of acute breathlessness is heavily reliant on investigations, such as blood-based biomarkers [e.g., C-reactive protein (CRP) and B-type natriuretic peptide] and radiological procedures. These biomarkers have clinical utility primarily in patients with single pathologies but have poor discriminatory power in patients with multifactorial presentations of acute breathlessness and are particularly challenging to interpret in the context of preadmission treatment exposure (e.g., antibiotics for pneumonia and admission CRP values) (*2*).

Breathomics, the characterization of volatile organic compounds (VOCs) in exhaled breath, enables the evaluation of diagnostic and prognostic biomarkers in acute breathlessness directly from the lung and incorporating metabolites from the systemic circulation (*3*). The assessment of exhaled, low-molecular weight biochemicals, chemically classified as VOCs, has been presented as a new paradigm for the development of rapid, noninvasive diagnostic and prognostic biomarkers. However, the scarcity of robustly powered clinical studies, combined with a lack of standardization in sample collection and analysis and data and chemometric processing, have delayed further translation of this technology to clinical settings.

Notwithstanding these challenges, the potential of breathomics is becoming increasingly recognized in research and therapeutic development in respiratory diseases. The emergence of powerful high-resolution mass spectrometry (MS) and multidimensional separation technologies, such as comprehensive two-dimensional gas chromatography coupled with MS (GC×GC-MS), which provides visual readouts of breath-based biomarkers (*4*, *5*), has facilitated research advances. Although chemometric analyses play a vital role in this field, the enhanced dimensionality of GC×GC-MS data enriches established chemometric and imaging-based characterization methods for visualizing, extracting, and quantifying VOC markers from complex and previously unresolved matrices.

[1]Department of Respiratory Sciences, University of Leicester, Leicester LE1 7RH, UK. [2]School of Chemistry, University of Leicester, Leicester LE1 7RH, UK. [3]School of Geography, Earth and Environmental Sciences, University of Plymouth, Plymouth PL4 8AA, UK. [4]Department of Chemistry, Loughborough University, Loughborough LE11 3TT, UK. [5]Leverhulme Centre for Demographic Science, University of Oxford, Oxford OX1 1JD, UK. [6]Nuffield College, University of Oxford, Oxford OX1 1NF, UK. [7]Department of Cardiovascular Sciences, University of Leicester, Cardiovascular Research Center, Glenfield General Hospital, Leicester LE3 9QP, UK. [8]Institute of Medical Science, University of Tokyo Shirokanedai, Minato-ku 4-6-1 108-8639, Tokyo, Japan. [9]Emergency Medicine Academic Group, Department of Cardiovascular Sciences, University of Leicester, University Road, Leicester LE1 7RH, UK. [10]National Heart and Lung Institute, Imperial College, London SW3 6LY UK.
*Corresponding author. Email: michael.wilde@plymouth.ac.uk (M.J.W.); s.siddiqui@imperial.ac.uk (S.S.)
†These authors contributed equally to this work as co-first authors.

Here, we present a real-world, prospective study of acutely unwell hospitalized patients presenting breathlessness due to severe exacerbations of cardiorespiratory etiology [asthma, chronic obstructive pulmonary disease (COPD), heart failure, or pneumonia] and healthy controls. By isolating and visualizing exhaled VOCs with GC×GC-MS, coupled with rigorous clinical phenotyping, exhaled breath metabolites were shown to have high diagnostic accuracy for severe cardiorespiratory exacerbations (including in the presence of diagnostic uncertainty) and to be dysregulated across several pertinent volatile classes in different clinical subtypes of cardiorespiratory exacerbation. This research provides pivotal evidence that shows how breath biomarker platforms may be used in acute care and demonstrates the potential for translation of this technology into a real-world clinical setting.

RESULTS

Participant demographics and clinical characteristics

As part of the East Midlands Breathomics Pathology Node (EMBER), exhaled breath from 277 participants recruited from acutely breathless hospitalized patients and matched healthy controls was sampled (Fig. 1). Sample size calculations are detailed in the Supplementary Materials and Methods ("sample size estimation") and table S1. Breath samples were analyzed to identify dysregulation of metabolic classes in cardiorespiratory disease and investigate whether exhaled VOC profiles could predict acute cardiorespiratory exacerbations despite diagnostic uncertainty and thus have a potential role in phenotyping acute cardiorespiratory breathlessness (fig. S1). Participants' mean (SD) age was 60.8 ± (16.8) years; Fifty-one percent were males. Thirty patients required supplemental oxygen on admission, and the mean admission modified early warning score (mEWS-2 score) was 2. The cohort was made up of patients presenting the following exacerbation subtypes: acute severe asthma (n = 65), acute severe COPD (n = 58), acute severe heart failure (n = 44), community acquired pneumonia (n = 55), and healthy volunteers (n = 55), recruited between May 2017 and December 2018. Participants' demographic and clinical characteristics are summarized in (Table 1). Breath samples were collected using a respiration collector for in vitro analysis (ReCIVA) device, adopting a standardized sampling and gated protocol that enriches alveolar volatiles (*6*), and analyzed using thermal desorption (TD) coupled to comprehensive GC×GC with dual flame ionization detection (FID) and MS.

Unbiased discovery using TDA identifies breath markers of acute disease

Topological data analysis (TDA) is an unsupervised machine learning tool used for the analysis of large-scale, high-dimensional, and complex datasets. It is highly sensitive to patterns that are often overlooked by other data reduction tools, such as principal components analysis (*7*).

TDA is a well-established data analytic technique for unbiased data-driven discovery–based phenotyping (*7*). TDA has proven to be a powerful tool, yielding critical insights in the prognostic phenotyping (*8*), cancer imaging biomarker stratification (*9*), disease classification using pathology biomarkers (*10*), and omics-based cancer phenotyping (*11*). Several publications have reported the use of TDA in the metabolomics field, for example, unbiased lipid phenotyping of lung epithelial lining fluid (*12*).

To achieve an unbiased discovery of exhaled VOCs predictive of the acute disease groups, patients were block-randomized post hoc into a discovery cohort of 139 participants (acute asthma, n = 33; acute COPD, n = 29; acute heart failure, n = 22; community acquired pneumonia, n = 28; and healthy volunteers, n = 27) and a replication cohort of 138 participants (acute asthma, n = 32; acute COPD, n = 29; acute heart failure, n = 22; community acquired pneumonia, n = 27; and healthy volunteers n = 28). Randomization allowed internal replication of diagnostic breath biomarkers while adjusting for relevant confounders. Details of the randomization and further clinical characteristics of the cohorts can be found in tables S2 to S3. Chemometric analysis and quantification of VOCs was performed blinded to clinical diagnosis by two analytical chemists (M.J.W. and R.L.C.), with biostatistical analyses linking subject identifier to chemometric biomarkers performed following data lock by an independent statistician (M.R.).

Eight hundred and five unique chromatographic features (peaks) were detected across the breath sample set using TD-GC×GC-FID/MS with 404 features detected on average in each sample. TDA applied to these 805 chromatographic features yielded topologically distinct networks that distinguished underlying causes of acute breathlessness while anchoring to corresponding blood-based biomarkers in both the discovery and replication cohorts (Fig. 2). Specifically, healthy volunteers and patients with acute heart failure formed distinct topological groupings in both discovery and replication populations. Respiratory admissions due to acute asthma, acute COPD, and pneumonia formed a topological continuum albeit within distinct regions of a single network in the replication cohort; similar findings were observed in the discovery cohort, with the exception of acute asthma forming a distinct grouping.

Breath biomarker clinical prediction scores

To create a concatenated list of exhaled breath biomarkers suitable for diagnostic application, we applied a threshold of 80% feature-presence per patient group, below which, features were removed to effectively reduce the number of features used in subsequent models with more than 20% of zero values for peak areas (fig. S2). We found that the zero-valued peak areas were randomly distributed across the disease groups in all but seven features. The exclusion of the seven features where there was some evidence that zero-valued peak areas were not randomly distributed across the disease groups did not alter the results of the regression models.

Further filtering steps using least absolute shrinkage and selection operator (LASSO) and elastic net regression methods, followed by removal of 38 peaks that were considered to be chemical and material artifacts (e.g., siloxanes), generated a final panel of 101 exhaled breath volatiles (tables S4 to S8). Therefore, the analysis plan permitted the identification of a rich and chemically diverse response in the VOC profile as opposed to only a handful of individual VOC markers and afforded the generation of biomarker scores. The data were examined for batch effects and were adjusted accordingly. Batch effects detected related to major instrument maintenance events, which occurred twice creating three groups. No contributions were observed on the basis of the ReCIVA device used, operator, time of day, or volume of breath sample collected, most likely nullified by the simultaneous and consecutive recruitment across all cohorts throughout the study to reduce potential biases (fig. S3 and S4).

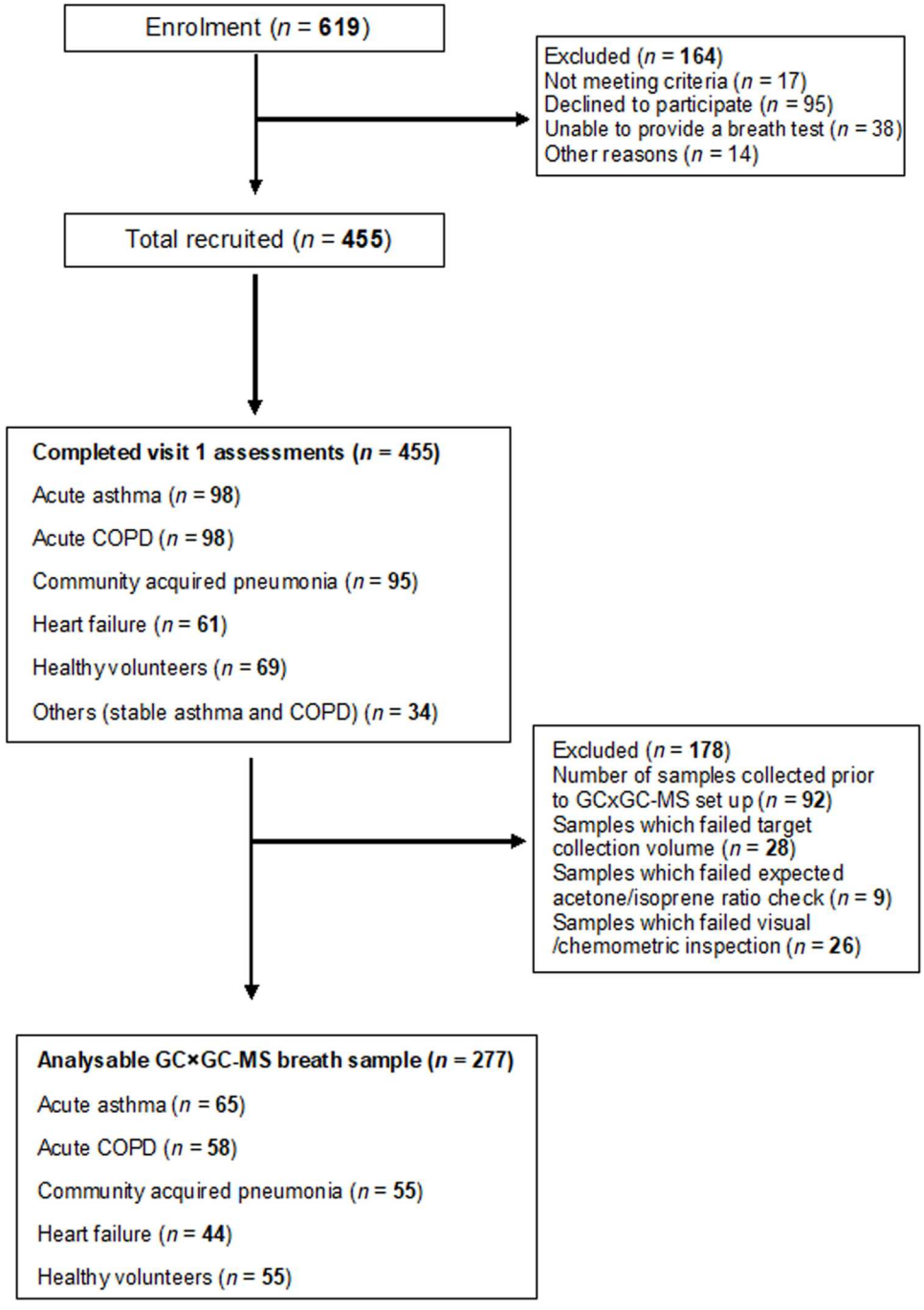

Fig. 1. Study CONSORT diagram. CONSORT diagram outlining the acute study recruitment and number of analyzable GCxGC-MS breath samples.

The value of the generated acute disease VOC biomarker score was found to be higher in acute cardiorespiratory patients compared to healthy volunteers (Fig. 3A). For the discovery cohort (n = 139), the acute disease VOC biomarker score effectively differentiated participants with acute cardiorespiratory exacerbations from age-matched healthy controls with an area under the curve (AUC) of 1.00, $P < 0.0001$, sensitivity of 1.00, specificity, positive predictive value (PPV) of 1.00, and negative predictive value (NPV). For the replication cohort (n = 138), the same VOC biomarker score differentiated participants with acute disease from healthy controls with AUC of 0.90 (0.83 to 0.96), $P < 0.0001$, sensitivity of 0.88 (0.82 to 0.94), specificity of 0.79 (0.63 to 0.94), PPV of 0.95 (0.91 to 0.99), and NPV of 0.51 (0.36 to 0.65) (Fig. 3B).

To evaluate the impact of potential confounders on our model classification, we reran our statistical models, adjusting for the following factors: (i) smoking status (current, ex-smoker, or never a smoker); (ii) time between hospital admission and the acquisition of the breath samples because this time period is often the period

Table 1. Demographics and clinical characteristics of study participants. Continuous variables are presented as means ± SD. Categorical variables are presented as numbers (%).

	Total number	Healthy controls	Acute asthma	Acute COPD	Pneumonia	Heart failure	*P* value
Total number of participants (*n* =)	**277**	**55**	**65**	**58**	**55**	**44**	
Demographics							
Age *, years	60.8 ± (16.8)	63.05 ± (11.78)	44.3 ± (17.93)	69.82 ± (8.16)	60.67 ± (16.50)	70.72 ± (11.04)	0.124
Gender male (*n* =) (%)	143 (51%)	26 (47%)	25 (38%)	33 (56%)	27 (49%)	32 (72%)	**0.008**†
Body mass index (BMI)*,‡	29.5 ± (7.3)	28.2 ± (4.5)	31.5 ± (9.0)	27.5 ± (7.7)	29.2 ± (6.9)	31.5 ± (6.5)	0.767
Smoking current smoker (*n* =) (%)	53 (19%)	4 (7%)	13 (20%)	21 (36%)	11 (20%)	4 (9%)	**0.001**†
Vital signs							
Temperature (°C)*	36.7 ± (0.6)	36.1 ± (0.4)	36.8 ± (0.5)	36.7 ± (0.5)	37.1 ± (0.7)	36.5 ± (0.3)	**0.000**
Heart rate (beats/min)*	87.2 ± (18.5)	68.1 ± (9.54)	99.6 ± (17.2)	92.9 ± (15.6)	90.3 ± (15.4)	81.3 ± (15.6)	**0.005**
Respiratory rate (breaths/min)*	18.9 ± (4.2)	13.0 ± (1.8)	20.5 ± (3.4)	21 ± (2.5)	20.4 ± (4.6)	19.1 ± (1.8)	**0.000**
Oxygen saturations (%)*	95.8 ± (3.0)	97.7 ± (1.3)	96.1 ± (2.5)	94.0 ± (2.9)	94.5 ± (0.5)	96.5 ± (1.9)	**0.001**
Systolic blood pressure (mmHg)*	131.5 ± (19.2)	134 ± (15.7)	133 ± (17.7)	133 ± (20.5)	126 ± (19.4)	128 ± (22.2)	0.515
Total mEWS-2 score§,‖	1 (0–3)	0 (0–1)	2 (1–3.5)	3 (1–5)	2 (1–3)	1 (0–2)	**0.000**
Breath sampling							
Time from admission to breath sampling (hours)§	16 (3.0–23.0)	1 (1–1)	16 (9.2–22.7)	18 (12.5–23.0)	18 (11.0–23.0)	23 (19.0–26.0)	0.000
Symptoms assessment							
Breathlessness VAS score (mm)*,¶	58.1 ± (31.6)	6.2 ± (9.3)	76.6 ± (14.2)	71.6 ± (19.2)	67.8 ± (22.1)	67.9 ± (20.0)	0.000**
Cough VAS score (mm) *,¶	43.3 ± (33.2)	8.7 ± (14.3)	64.5 ± (26.7)	57.8 ± (27.0)	53.6 ± (30.6)	24.3 ± (25.2)	0.000**
Wheeze VAS score (mm) *,¶	41.8 ± (34.9)	3.4 ± (6.4)	66.2 ± (24.5)	60.3 ± (29.0)	45.1 ± (34.8)	28.1 ± (28.6)	0.000**
eMRC# score (*n* =) (%)							
1	17 (6%)		1 (1.5%)	8 (13%)	7 (12%)	1 (2%)	0.000†
2	6 (2%)		0 (0%)	0 (0%)	5 (9%)	1 (2%)	0.000†
3	15 (5%)		6 (10%)	0 (0%)	7 (12%)	2 (4.5%)	0.000†
4	50 (18%)		16 (25%)	11 (19%)	6 (11%)	17 (38.5%)	0.000†
5a	112 (40%)		38 (51%)	32 (55%)	22 (41%)	20 (46%)	0.000†
5b	21 (7%)		3 (4.5%)	7 (13%)	8 (15%)	3 (7%)	0.000†
Exposure to antibiotics and steroids within 2 weeks of hospital admission							
Antibiotics (*n* =) (%)	61	*n* = 0 (0%)	*n* = 24 (36.9%)	*n* = 23 (39.6%)	*n* = 10 (18.2%)	*n* = 4 (9.0%)	0.002†
Steroids (*n* =) (%)	57	*n* = 0 (0%)	*n* = 28 (43.0%)	*n* = 24 (41.3%)	*n* = 3 (5.4%)	*n* = 2 (4.5%)	0.000†
Morbidity and mortality measures							
Length of hospital stay (days)§	3 (2–6)		2.0 (1.0–3.0)	4.0 (2.0–6.0)	4.0 (2.0–5.0)	7.0 (4.0–11)	0.000**
30 to 60 days hospital readmission (*n* =)	29		7	9	6	7	0.461†
1-year all-cause mortality	12	0	1	5	1	5	0.078†
Laboratory parameters							
C-reactive protein (mg/liter)§	11 (5.0–34.2)	5 (5–5)	10.0 (5.0–23.0)	12.0 (5.0–20.7)	108.0 (53.5– 245.3)	11.0 (5.0– 22.0)	0.000**
Blood eosinophil count 109/liter§	0.13 (0.06–0.24)	0.17 (0.09–0.24)	0.18 (0.06–0.42)	0.13 (0.06–0.24)	0.08 (0.04–0.14)	0.13 (0.08–0.23)	0.000**
Troponin T (ng/liter)§	3.3 (1.0–11.4)	2.05 (1.0–2.7)	1.55 (1.0–3.4)	3.75 (2.6–10.9)	4.3 (2.18–11.3)	20.2 (13.4–59.6)	0.000**

continued on next page

	Total number	Healthy controls	Acute asthma	Acute COPD	Pneumonia	Heart failure	*P* value
BNP (ng/liter)§	40.5 (20.6–98.9)	28.40 (17.60–39.88)	20.4 (12.1–40.0)	56.3 (24.3–95.0)	56.3 (27.4–132.1)	611.8 (172.1–1259.1)	0.000**
Questionnaires							
Asthma Quality of Life Questionnaire (AQLQ) total*	65		117.3 ± (37.3)				
COPD Assessment Test (CAT) *	58			26.7 ± (7.3)			
COPD decaf score *	58			1.7 ± (0.8)			
CURB65 score§	55				2 (1–3)		
NYHA score§	44					2 (1–3)	

*Data are expressed as means (SD) or *n* (%) ± (SD). †Pearson chi-square and Fisher's exact test. ‡The body mass index (BMI) is the weight in kilograms divided by the square of the height in meters. §Data expressed as median (interquartile range). ||Modified early warning score-2 is a guide widely used by medical services to determine the degree of illness of a patient based on their vital signs including respiratory rate, oxygen saturations, temperature, blood pressure, and heart rate. Vital signs were collected at the point of admission for acute disease groups. ¶Participants were asked to determine their degree of breathlessness, cough, and wheeze on a 100-mm VAS on admission. Higher scores indicate worse symptoms. #Extended Medical Research Council (eMRC) scale is a validated measure of perceived respiratory disability, scored from 1 to 5b. Higher scores indicate worse disability. *Kruskal-Wallis test comparing nonparametric data. ANOVA was used to assess the differences between groups for normally distributed continuous variables and Kruskal-Wallis for nonparametric continuous variables. Pearson chi-square and Fisher's exact were used to assess the differences in categorical variables. The results were considered statistically significant at *P* values <0.05.

within which acute treatments are delivered; (iii) the mEWS-2, which is a composite acuity score combining respiratory rate, oxygen saturations, systolic blood pressure, heart rate, degree of consciousness, confusion, and body temperature for each patient; and (iv) prior exposure to either antibiotics or steroids for cardiorespiratory illness in the fortnight before the index admission. We observed improved diagnostic accuracy in the replication cohort (AUC of 1.00, $P < 0.0001$) when considering these adjustments, which would be expected with the inclusion of acuity markers for the classification of acute illness.

Following a clinical adjudication process ("Clinical adjudication" section in Materials and Methods), each patient was assigned a degree of clinical diagnostic uncertainty using a 100-mm visual analog scale (VAS) at the point of clinical triage (Fig. 3C). Diagnostic uncertainty was defined as patients with values higher than or equal to the upper quartile of 20 mm on the VAS. The acute disease VOC biomarker score was able to identify acute disease with an AUC of 0.96 (0.92 to 0.99), $P < 0.0001$, sensitivity of 0.90 (0.82 to 0.97), specificity of 0.92 (0.85 to 0.99), PPV of 0.93 (0.86 to 0.99), and NPV of 0.89 (0.81 to 0.97) (Fig. 3D).

Exhaled breath biomarker disease-specific scores correlate with blood-based biomarkers and admission observations

As previously described, VOC biomarker scores were generated for each of the acute disease subgroups and healthy subjects without cardiorespiratory breathlessness. There was a weak but positive correlation in the combined discovery and replication cohorts ($n = 277$) between the VOC subgroup scores for pneumonia and CRP [$n = 277$, correlation coefficient (r) = 0.33, and $P < 0.0001$] and acute heart failure and brain natriuretic peptide (BNP; $n = 277$, $r = 0.33$, and $P < 0.0001$), in addition to a negative correlation between the healthy-state VOC score and CRP and BNP ($n = 277$, $r = -0.15$, $P < 0.0001$, and -0.21, $P < 0.0001$, respectively; Fig. 4A). Correlations were also identified between the acute disease VOC score and vital observations carried out during triage (Fig. 4B). The acute disease VOC score was also associated with 2-year all-cause mortality but not with the risk of 60-day readmission (fig. S5).

Diagnostic accuracy of breath biomarker scores in cardiorespiratory disease subgroups

A multinomial regression model using elastic net regularization was fitted to the matrix of 101 breath biomarkers with the 10-fold cross-validation repeated 1000 times. Linear combinations of the most stable features from the multinomial regression model fitted to the 101 biomarkers formed a set of scores for predicting probability of belonging to the different disease groups (acute asthma, acute COPD, pneumonia, heart failure, or healthy volunteers).

The overall classification accuracy for the statistical model generated from 101 breath biomarkers was assessed by comparing the balanced accuracy of model trained using the true class labels versus the balanced accuracy of the same model tested using randomly shuffled class labels. This process was repeated 1000 times. The balanced accuracy reported in fig. S6A shows the acute disease biomarker score in the discovery cohort. Figure S6B shows the acute disease biomarker score in the replication cohort, and fig. S6C reports the overall accuracy for the model using multinomial biomarker scores for the five subgroups (acute asthma, acute COPD, heart failure, pneumonia, and healthy volunteers). Replication was not evaluated in the subgroups because the study was not powered to do this.

For the pooled cohort ($n = 277$), the overall classification accuracy using all five biomarker scores was 0.72 [95% confidence interval (CI), 0.67 to 0.77]. The balanced accuracy was 0.83 for acute asthma, 0.78 for acute COPD, 0.80 for heart failure, 0.79 for community acquired pneumonia, and 0.93 for healthy controls (fig. S6).

Further comparative receiver operating curve (ROC) analyses were performed on the basis of the observed separation of asthma from pneumonia/COPD acute groups and heart failure from other acute exacerbation groups in the discovery and replication TDA analyses. The diagnostic AUC accuracies of the asthma biomarker

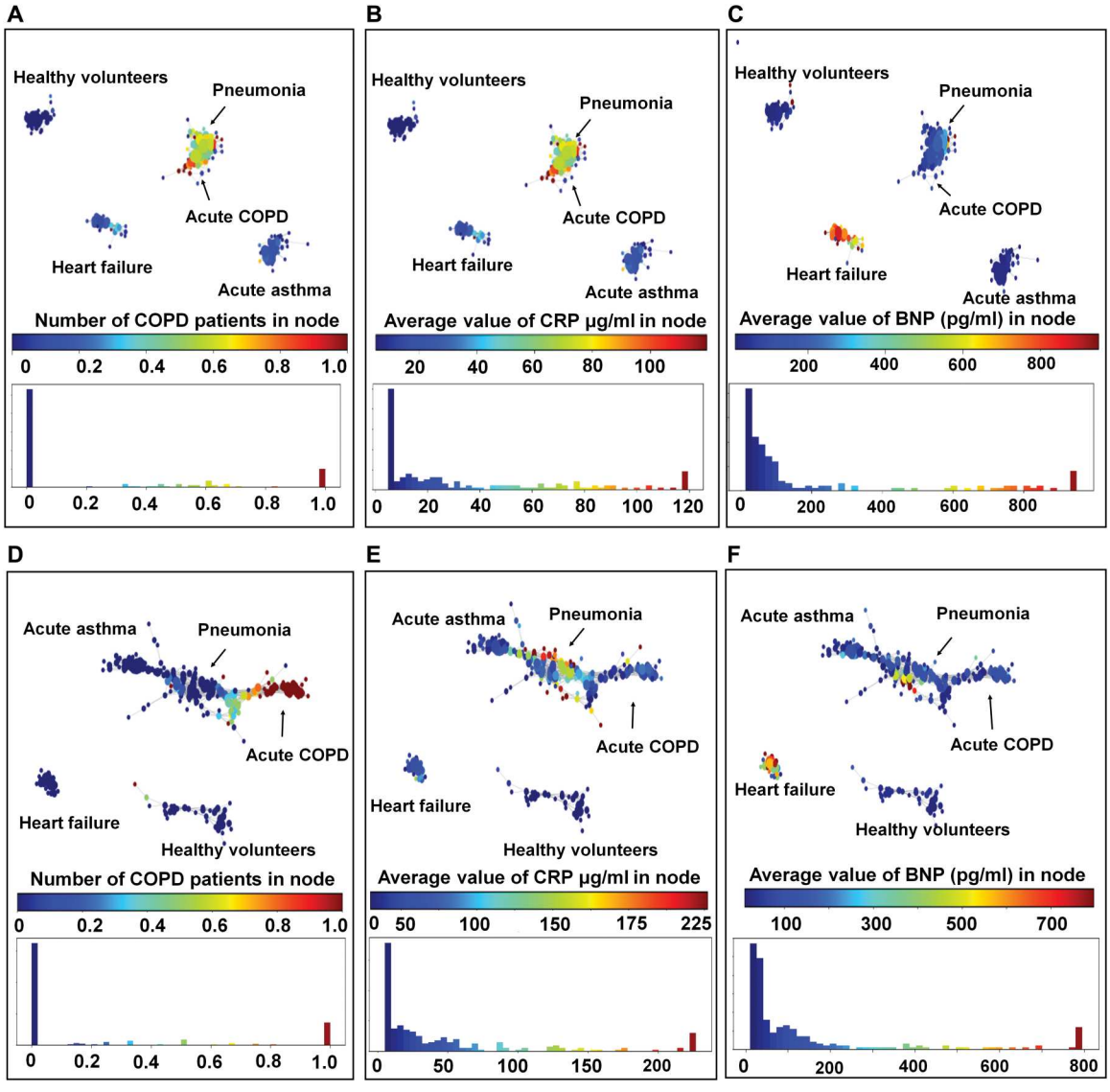

Fig. 2. TDA representing the various acute disease groups annotated by blood biomarkers. Each circle or "node" in the TDA graph represents a subject or group of subjects. Similar subjects are grouped together in the same node, and the relative similarity of the subjects is represented by the proximity of the nodes. The size of each node is determined by the number of subjects within it. (**A**) Visual mapping of the acute disease groups in the discovery cohort ($n = 139$) based on the discriminatory 805 features and colored by proportion of acute COPD exacerbations in each node. (**B**) The network is color-coded by the average values of CRP in each node in the discovery cohort ($n = 139$). Higher CRP values corresponded topologically with the COPD and pneumonia patients. (**C**) The network is color-coded by the average values of BNP in each node in the discovery cohort ($n = 139$). Higher BNP values corresponded topologically with the patients with heart failure. (**D**) The network is colored by proportion of acute COPD exacerbations in each node in the replication cohort ($n = 138$). In replication cohort, pneumonia and COPD exacerbation subjects occupied polar ends of the same TDA network. (**E**) The networks are colored by the average values of CRP in each node. High CRP values corresponded topologically with the pneumonia subjects. (**F**) The networks are colored by the average values of BNP in each node. High BNP values corresponded topologically with the heart failure subjects.

score against pooled pneumonia and COPD cohorts were AUC, 0.70 (0.62 to 0.78; $P < 0.0001$); sensitivity, 0.72 (0.64 to 0.83); specificity, 0.64 (0.55 and 0.73); PPV, 0.54 (0.43 to 0.64); and NPV, 0.80 (0.72 to 0.88). ROC analyses to assess the diagnostic value of the heart failure biomarker score against other acute disease groups were AUC, 0.78 (0.70 to 0.86) $P < 0.0001$; sensitivity, 0.77 (0.64 to 0.89); specificity, 0.71 (0.64 to 0.78); PPV, 0.40 (0.29 to 0.50); and NPV, 0.92 (0.88 to 0.97) (fig. S7).

The median values of the exhaled breath VOC scores and their distribution across disease subgroups are detailed in (fig. S8). Figure S9 is a Venn diagram demonstrating the distribution of the final panel of 101 exhaled breath biomarkers across the different disease groups.

We also ran our models adjusting for the following factors: (i) smoking status (current, ex-smoker, or never a smoker); (ii) time between hospital admission and the acquisition of the breath samples because this time period is often the period within which acute treatments are delivered; (iii) the mEWS-2, which is a composite acuity score combining respiratory rate, oxygen saturations, systolic blood pressure, heart rate, level of consciousness, and

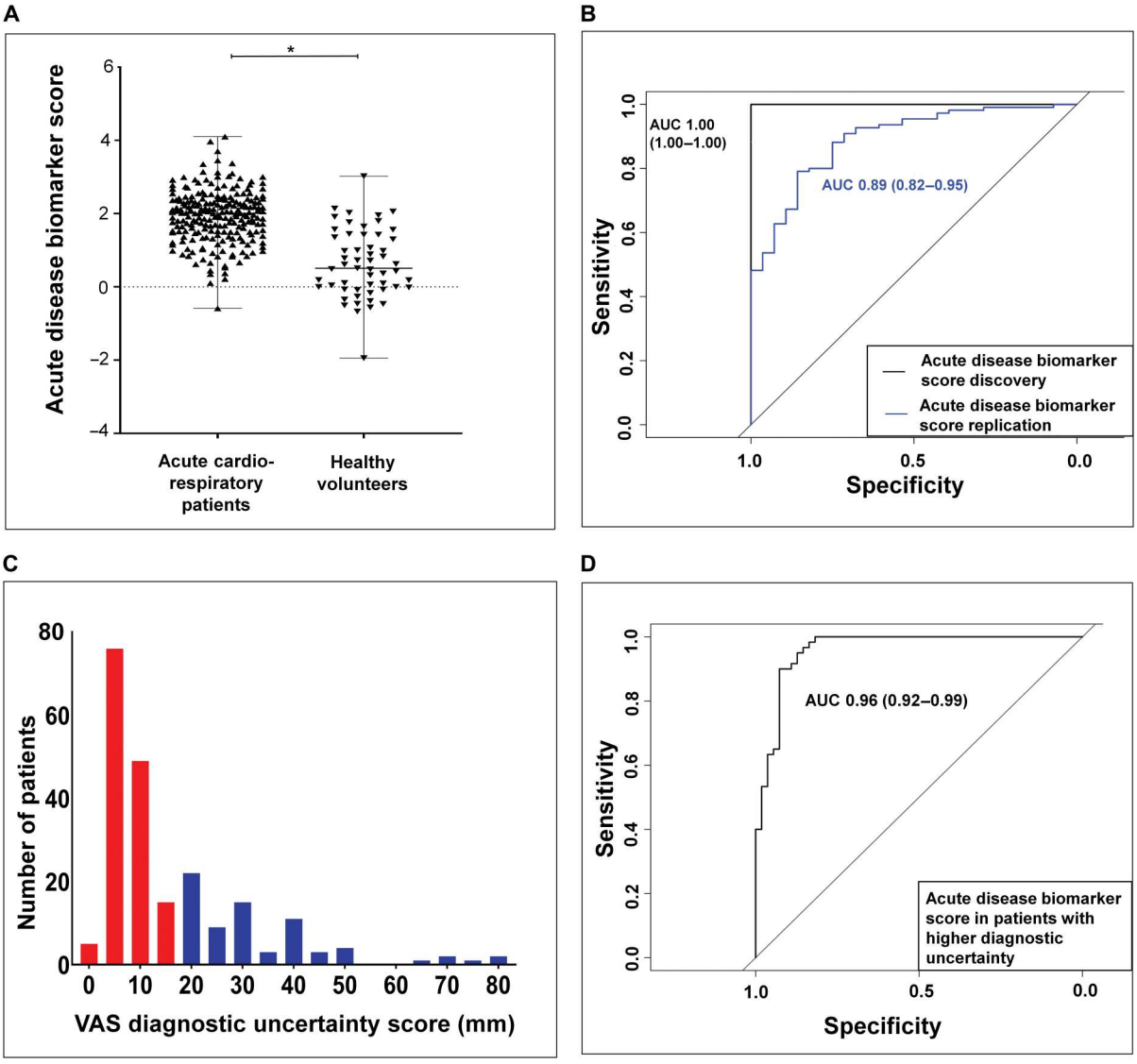

Fig. 3. Diagnostic accuracy of an acute VOC biomarker score. (**A**) Scatterplot demonstrating significant difference between breath VOC biomarker score values in acute cardiorespiratory patients compared to healthy volunteers. The black horizontal line within the scatterplot represents the median value of the biomarker score. Mann-Whitney test, *$P < 0.0001$. (**B**) Receiver operating characteristic (ROC) curve of participants in the discovery (black line, AUC of 1.00) and replication [blue line, AUC of 0.89 (0.82 to 0.95)] cohorts ($P < 0.0001$). (**C**) Histogram showing the number of patients with higher diagnostic uncertainty (blue bars with values greater than upper quartile value of 20 mm). (**D**) ROC curve assessing the discriminatory power of exhaled breath VOCs in participants with higher diagnostic uncertainty. AUC, 0.96 (0.92 to 0.99; $P < 0.0001$).

confusion for each patient; and (iv) prior exposure to either antibiotics or steroids for cardiorespiratory illness in the fortnight before the index admission. We observed only marginally improved diagnostic accuracy: acute asthma, AUC of 0.88 (0.831, 0.933; $P < 0.0001$); COPD, AUC of 0.86, (0.808, 0.918; $P < 0.0001$); heart failure, AUC of 0.91 (0.849, 0.969; $P < 0.0001$); community acquired pneumonia, AUC of 0.91 (0.863, 0.953; $P < 0.0001$); and healthy controls, AUC of 1.0, suggesting limited confounding influence of disease acuity on our biomarker scores (data file S1). Replication was not performed in the subgroups because the EMBER study was not powered for disease subgroup diagnostic accuracy.

Chemical classification of predictive markers in disease groups

Chemical identification of the 101-biomarker panel involved comparison with an authentic reference compound in accordance with the Metabolomics Standard Initiative (MSI) level 1 criteria for metabolite identification. The most common chemical classes associated with acute breathlessness in this study included straight-chain and methyl-branched hydrocarbons (30%), ketones (10%), aldehydes (8%), and terpenes (13%), followed by sulfur-containing VOCs (7%), alcohols (6%), aromatics (5%), esters (3%), nitrogen-containing VOCs (3%), ethers (2%), halogen compounds(1%), and an assortment of other less prevalent and less relevant classes, such as acrylates (12%) (table S9).

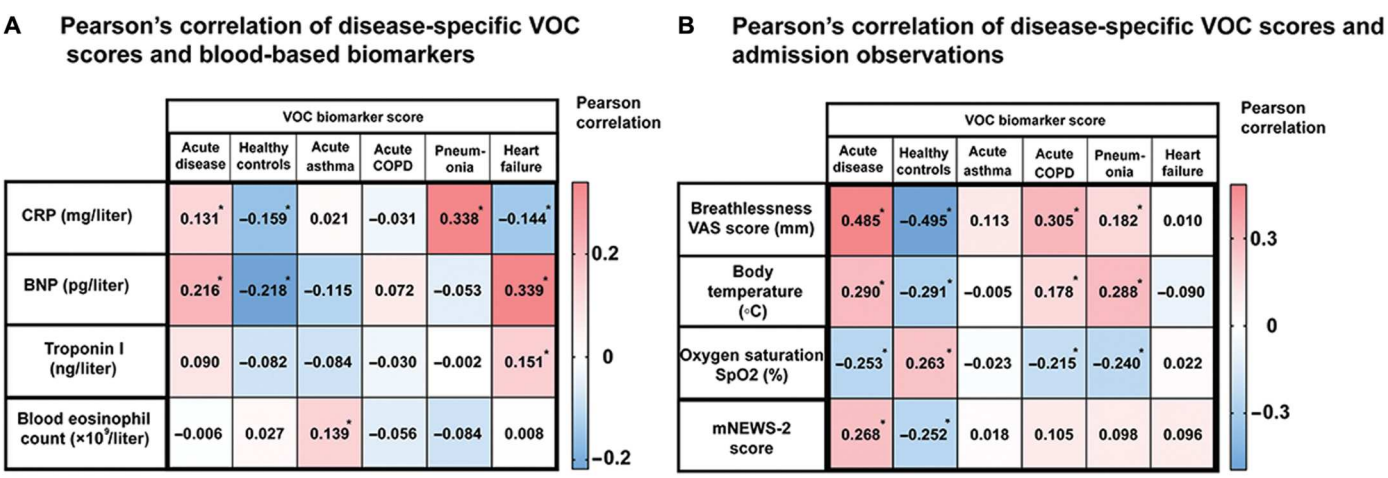

Fig. 4. Correlation of VOC biomarker score with blood biomarkers and disease acuity. (**A**) Pearson's correlation of disease-specific VOC scores and blood-based biomarkers. Pearson correlation demonstrating the positive and negative correlations between breath VOC scores and blood-based biomarkers. *$P < 0.05$. (**B**) Pearson's correlation of disease-specific VOC scores and admission observations. Pearson correlation between the VOC biomarker score and admission vital signs. VAS, visual analog scale (100 mm); participants were asked to rate their breathlessness on a 100-mm VAS on admission.

Metabolite set enrichment and chemical similarity analysis

Unlike functional indications, which are reliant on mapping metabolites with known, well-annotated metabolic pathways, metabolic changes indicative of response can be derived independently. To derive clues of responsive indication, the panel of 101 features was assessed for covarying clusters (i.e., metabolite sets).

Metabolite sets were derived on the basis of Ward hierarchical cluster analysis using the ChemRICH method reported previously (Fig. 5A and fig. S10) (*13*), and broader communities were derived from Louvain cluster analysis (Fig. 5B and tables S10 to S13) to help interpret the correlation graphs. Overall, 20 metabolite sets were identified using ChemRICH, 11 of which were enriched during acute cardiorespiratory exacerbations. The seven metabolite sets that were up-regulated consisted of predominantly acyclic and branched hydrocarbons (sets 3, 5, 7, and 9 in fig. S10). The results from the analysis here demonstrated enriched coexpression of hydrocarbons with high chemical similarity providing primary evidence of exhaled VOCs indicative of disease response measured in vivo. This is clearly seen in Fig. 5A, with the metabolite sets (inner tree) labeled by broader chemical classifications (outer ring); C5-7, C8-10, and C11-16 form clusters based on carbon number also exhibiting the highest change during acute exacerbation. Owing to the increased separation power afforded by GC×GC-MS, it was possible to map the VOC signatures back to the multidimensional chromatograms for the visualization of exhaled breath metabolites, which revealed distinct diagnostic signatures for acute cardiorespiratory breathlessness (Fig. 5C).

DISCUSSION

In this pragmatic, acute-care study, we evaluated the validity of breath biomarker profiling in high-acuity patients presenting acute cardiorespiratory breathlessness. Using GC×GC-MS, we observed that robust and validated sampling of alveolar breath coupled with GC×GC-MS biomarker characterization demonstrated high diagnostic accuracy for acute cardiorespiratory exacerbations.

We have also identified putative biomarker scores from subsets of breath VOC biomarkers that classify cardiorespiratory exacerbation subtypes and warrant validation in appropriately powered replication studies. Furthermore, we have identified several classes of VOCs that are highly correlated and selectively enriched or suppressed in acute disease (including subgroups) compared to health, providing potential insights into broad dysregulation of the metabolome in acute cardiorespiratory exacerbations.

The analytical methods described here were underpinned by robust biomarker development protocols using TD-GC×GC-FID/MS, integral to the standardization and integration of breath analysis in large translational studies (*5*, *14*). Several potential confounders, including batch variation were addressed in detail. Furthermore, biomarker quantification of the 101 VOCs followed the recommendations of the MSI, with 58 compounds identified against pure and traceable standards (level I), 21 putative identities based on mass spectral and retention index library matches (level 2), and 22 classified on mass spectral data (*15*). Markers that appeared to localize to individual cardiorespiratory conditions could be readily visualized using TDA.

The identification of hydrocarbons and carbonyls as the major chemical classes was consistent with current mechanistic understanding, postulated as chemical end points of lipid peroxidation resulting from oxidative stress during inflammation. Aldehydes such as nonanal, decanal, and hexanal were predictive for asthma; ketones included 2-pentanone (asthma), cyclohexanone (pneumonia), and 2,3-butanedione (COPD), which were all previously reported (*4*, *16*–*20*). Individual hydrocarbons, such as 2,4- and 2,2-dimethylpentane, 2-methylbutane, 4-methyldecane, 5-methylnonane, and isoprene have been previously reported as predictive for pneumonia and heart failure (*18*, *21*). Sulfur-containing VOCs, such as 3-methylthiophene, allyl methyl sulphide, and carbonyl sulphide (found to be predictive of COPD) are associated with bacterial metabolism, postulated to originate from the gut (*22*) and, on occasions, as a result of radiation injury (*23*); however, 2,3-butanedione, also predictive of COPD, has been identified as a metabolic product of bacterial isolates from patients with

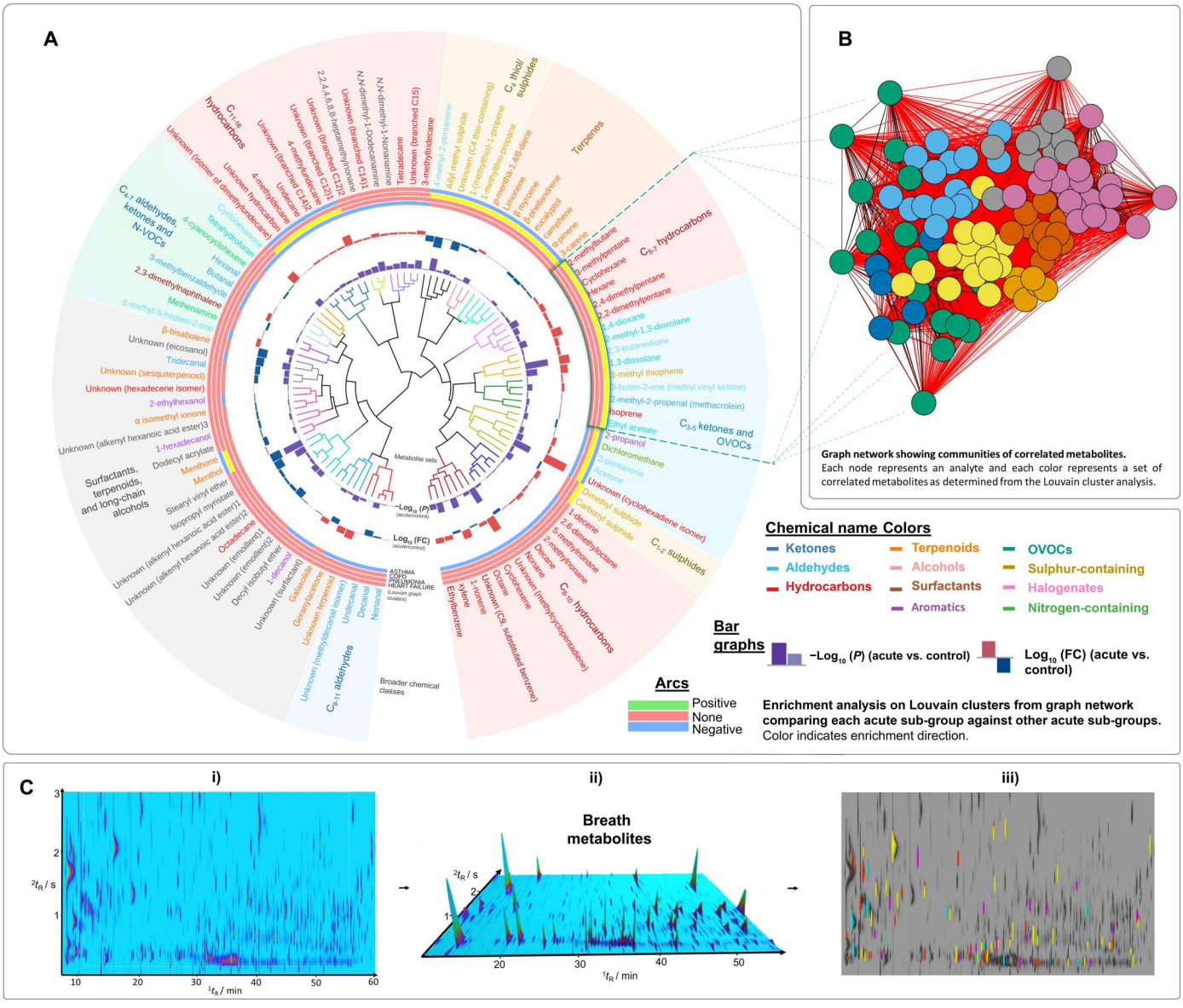

Fig. 5. VOC biomarker chemical enrichment in acute cardiorespiratory exacerbations. (**A**) Circular correlation tree generated on the basis of metabolite set enrichment and chemical similarity analysis of 101 breath volatiles associated with acute breathlessness. Branches depict metabolite sets derived using the ChemRICH; bar graphs portray $-\log_{10}(P)$ and $\log_2$ (fold change) values of 101 features extracted using LASSO regression (table S4) in acute breathlessness compared with control group. The arcs represent the Louvain clusters, derived from the correlation graph (green for up-regulated, red for not significant, and blue for down-regulated according to K-S test result). Chemical names are colored on the basis of their chemical classification and colored regions used to summarize broader chemical groups. (**B**) Correlation graph showing metabolite communities identified using Louvain clustering, with the identity and location of the cluster enriched in heart failure projected onto the circular dendrogram. (**C**) (i) Example GC×GC chromatogram showing complex profile of breath metabolites, (ii) three-dimensional render of chromatogram showing visualization of breath markers, and (iii) phenotypic differences based on features included in the breath biomarker scores (table S9) (yellow, asthma; red, pneumonia; magenta, COPD; and cyan, heart failure). Created in part using the iTOL online https://itol.embl.de/.

cystic fibrosis (CF) (*22*) and postulated to be an important metabolite in monitoring lung infection in CF, COPD, and pneumonia. We acknowledge that the biological origin of most VOCs within our biomarker signature has yet to be fully elucidated. Future studies combining carbon labeling of glucose with in vitro headspace analysis of primary cells will be required to more precisely establish the molecular origins of VOCs identified in this report.

Not all compounds were considered to be endogenous VOCs, with 27 possibly attributed to potential cosmetics. Eleven of the features predictive of the control group were assigned as either possible fragrances (e.g., α isomethyl ionone) or waxy long-chain chemicals used in cosmetics as emollients and surfactants (e.g., stearyl vinyl ether and isopropyl myristate). These may have been captured in the breath sample because of the proximity of the sorbent tubes to the patients' faces. A frequent problem with ascribing the

origin of VOCs is that those compounds often identified in cosmetics are natural products; therefore, there is uncertainty about the precise origin of these makers. The down-regulation in acute disease of several of these markers may be indicative of them being biomarkers as opposed to exogenous confounders from cosmetics.

Coexpression and enrichment analysis of the Louvain clusters on the correlation graph revealed a set of highly correlated metabolites notably enriched in specific disease groups. Comparison of the Louvain clusters with the metabolite sets identified using the method previously described (*13*) demonstrated strong overlap. The metabolites enriched in heart failure were a cluster of highly correlated $C_{5\text{-}7}$ hydrocarbons and $C_{3\text{-}5}$ carbonyls with high chemical similarity (based on Tanimoto coefficients as determined in fig. S10). The cluster included 2,4- and 2,2-dimethylpentane, 2-methylbutane, 2-methyl-1,3-butadiene (isoprene), 3-methylpentane, hexane, and cyclohexane. These hydrocarbons (2,4- and 2,2-dimethylpentane, 2-methylbutane, and isoprene) have been individually reported and associated with heart failure and pneumonia (*17*, *20*). However, the analysis here captured the collective response and demonstrated enriched coexpression of these hydrocarbons.

The analysis also revealed a separate set of highly correlated aldehydes (nonanal, decanal, undecanal, and a methyldecanal isomer), found to be potentially depleted in acute exacerbations of asthma compared with acute exacerbations of COPD and pneumonia. Depletion of VOCs during in vitro experiments has been reported as a consequence of metabolic activity by immune cells (*24*–*26*), but the association here is tentative and should be interpreted with caution because of the correlation between inhaled air and exhaled air concentrations of these compounds (median Spearman rank = 0.60), also previously observed (*27*).

Our study has some limitations. Although internally replicated, the results presented here for acute VOC biomarker scores and cardiorespiratory exacerbation subtype biomarker scores are limited by the lack of external replication and internal replication, respectively. The single center design of this study may have introduced nonpathogenic biases related to diet, environment, and lifestyle that might be absent in a multicenter study. The cardiorespiratory exacerbation disease subgroups preselected in this study were chosen as the commonest reported causes of cardiorespiratory breathlessness (*28*, *29*), and there was a relatively high degree of clinical certainty in the diagnostic labels. For these findings to be generalizable, the identified markers will need to be validated in unselected cardiorespiratory populations and patients presenting mixed acute pathologies.

In conclusion, we have conducted an acute care volatile breath biomarker study using robust clinical and analytical technology and have identified biomarkers with high combined diagnostic sensitivity and specify in acute cardiorespiratory disease. In addition, we have used methods enabling robust biomarker identification and mechanistic association. Future clinical studies in acute cardiorespiratory patients at initial presentation and triage using near patient sensor platforms capable of detecting the volatiles identified here are warranted to maximize the clinical impact of our discovery biomarker approach.

MATERIALS AND METHODS

Study design

The study design, eligibility criteria, and methodology have been described in detail previously (*30*). This is a prospective, real-world, observational study (ClinicalTrials.gov Identifier NCT03672994), carried out in a tertiary cardiorespiratory center in Leicester, United Kingdom. Participants were recruited year-round from May 2017 through to December 2018.

Patients with self-reported acute breathlessness, requiring admission and/or a change in baseline treatment, presenting within University Hospitals of Leicester (UHL) were approached for study participation. After triage and senior clinical assessment, if a primary clinical diagnosis of (i) acute decompensation of heart failure, (ii) exacerbation of asthma/COPD, or (iii) adult community acquired pneumonia was suspected by the triage nurse/attending clinician at triage, then members of the research team would evaluate patients against predefined eligibility criteria for study participation.

A total of 277 participants were included in the final analysis. Sample size attrition from the recruited 455 participants is detailed in (Fig. 1). This was mainly due to the delayed deployment of GC×GC-MS and analytical quality control/quality assurance (QC/QA). These decisions were made objectively during the discovery phase of the program, prioritizing the optimization of a robust sampling and analysis pathway. Sample size calculations were informed on the basis of estimation for adequate sensitivity and or specificity as detailed in (table S1).

The 277 subjects were randomized post hoc to Discovery and Replication cohorts in a 1:1 ratio through block random assignment. Randomization was stratified on the basis of (i) adjudicated clinical diagnosis, (ii) time to breath-testing from the point of hospital admission, and (iii) clinical diagnostic uncertainty score. The R package randomizr was used to perform block random assignment. After block randomization, there were 139 and 138 subjects in the discovery and replication sets respectively.

Inclusion and exclusion criteria and study objectives are outlined in detail in "Study design" and "Study objectives" sections of the Supplementary Materials. Informed consent was obtained in all participants within 24 hours of hospitalization. Age- and/or home environment–matched healthy volunteers were recruited. Where environment-matched controls were unsuitable, healthy volunteers were recruited from local recruitment databases and via advertising. Healthy volunteers were defined as participants with no prior history of asthma, COPD, and heart failure and had not been admitted to the hospital with community-acquired pneumonia within 6 weeks of the baseline study visit. The diagnostic accuracy of the reported exhaled breath VOCs was tested following the Standards for reporting of Diagnostic Accuracy Studies guidelines (table S14) (*31*). Statistical procedures presented here were carried out as complete case analysis with no imputations. Transparent Reporting of multivariate prediction model for Individual Prognosis or Diagnosis (TRIPOD) was followed for multivariate prediction models (table S15) (*32*, *33*).

The trial was conducted in accordance with the ethics and principles of the deceleration of Helsinki and Good Clinical Practice Guidelines. All patients provided written consent. The National Research Ethics Service Committee East Midlands has approved the

study protocol (REC number: 16/LO/1747). Integrated Research Approval System (IRAS) 198921.

Clinical adjudication

A clinical adjudication process was introduced to precisely define and quantify the diagnostic labels in the study, addressing any potential misclassification. A panel of two senior clinical adjudicators (S.S. and N.J.G.) reviewed all available case notes and imaging and determined the primary diagnosis for each case by discussion to reach a concordance. The degree of diagnostic uncertainty was marked on a 100-mm VAS scale, blinded to given diagnosis and blood biomarkers.

The process was implemented with emphasis on mirroring an acute triage pathway, where all pathology data required to support the diagnosis, e.g., CRP and BNP, are not available at the initial clinical review. The degree of diagnostic uncertainty obtained from the clinical adjudication process was factored into the block randomization, and subjects with higher diagnostic uncertainty (≥upper quartile = 20 mm) were assessed separately as previously described (Fig. 3, C and D).

Breath collection and analysis

Collection of breath samples

Exhaled breath collection was attempted in all consented participants using a Conformitè Europëenne (CE)-marked breath sampling device RECIVA (Owlstone Nanotech Ltd.), in combination with a dedicated clean air supply unit (*34*). Breath sampling was well tolerated by all participants (*6*).

Sample storage and preparation

Samples were dry-purged on arrival for 2 min using nitrogen (chemically pure grade with inline trap, BOC) at a flow rate of 50 ml min^{-1} and then stored in refrigeration at 2°C until analysis. Before analysis, samples were left to reach room temperature before being spiked with a 0.6-μl aliquot of 20 μg ml^{-1} standard solution containing deuterated toluene and octane, into a flow of nitrogen at a flow rate of 100 ml min^{-1} for 2 min, purging the excess solvent.

Exhaled breath analysis

Breath samples were analyzed by TD with comprehensive GC×GC using flow modulation and coupled to dual FID and MS. Dual detection, with the use of MS and FID, uses the excess flow from the flow-based modulator suited for volatile analyses, providing both quantitative and qualitative results.

Analysis by GC×GC was optimized and conducted as described previously (*5*) using an Agilent 7890A gas chromatogram, fitted with a capillary flow technology (CFT) flow modulator and 5799B mass spectrometer with a high-efficiency electron ionization (EI) ion source (Agilent Technologies Ltd.). The instrument was coupled to a TD-100xr TD auto-sampler (Markes International Ltd.). Samples were analyzed in trays; typically, six per tray along with a reference mixture containing *n*-alkanes and aromatics run every tray, and a reference indoor air VOC mixture run every four trays. Data were acquired in MassHunter GC-MS Acquisition B.07.04.2260 (Agilent) and processed (i.e., baseline correction, alignment, and feature extraction) with a workflow previously developed and optimized, using GC Image v2.8 suite (GC Image, LLC.) and Python (*14*). The sorbent tubes used were Tenax/TA with Carbograph 1TD (Hydrophobic, Markes International Ltd.) with matching cold trap. Chromatographic features arising from analytical artifacts were removed from the peak table. (e.g., ubiquitous siloxanes). For purposes of quality control, samples were analyzed in accordance with a previously published workflow, and a detailed sample history, metadata, and experimental data were recorded at every stage of the collection and analysis using the open-access LabPipe toolkit (*5*, *35*).

Chemical speciation of identified breath biomarkers

The chemical nature of volatile metabolites exhaled in breath comprises a diverse mixture of non-novel, low-molecular weight compounds. Thus, for most features, chemical identification involved comparison with an authentic reference compound in accordance with the MSI Level 1 criteria for metabolite identification outlined in table S9. Identification was based on a minimum of two independent and orthogonal identifiers, including primary and secondary retention time, mass spectral similarity match, and calculated retention index. When an authentic reference compound was unavailable, chemical identification was compliant with MSI level 2 for putative annotations. The highly structured chromatographic data and group-type separation afforded by GC×GC, alongside a well-characterized chromatographic space from analyzing an extensive library of authentic compounds, gave increased confidence in the tentative assignments made. The orthogonal separation of GC×GC also meant that chemical identification of unknown metabolites could be made, at minimum, in compliance with MSI level 3 for putative chemical classification.

Sample analysis QC/QA procedures

For purposes of quality control, samples were analyzed in accordance with a previously published workflow, and a detailed sample history, metadata, and experimental data were recorded at every stage of the collection and analysis using the open-access LabPipe toolkit (*35*). The chromatographic method was optimized for peak shape, sensitivity, and separation; quality control charts of the internal standards were used to track the stability of the TD-GC×GC-FID/MS analysis, and instrument performance was evaluated after the assessment of the variation of retention times, peak area, and shapes of VOCs in two standard reference mixtures every six samples (*5*). Before being conditioned and sent to clinic, the number of heat cycles and weight for each tube was recorded to monitor tube age and integrity. For each conditioning cycle, all tubes were given a batch number, and a batch blank was analyzed to monitor contamination from the beginning of the sample preparation process. Furthermore, all batches were given an expiry of 2 weeks to ensure routine monitoring.

To minimize the influence of biological and analytical confounders (e.g., circadian rhythm and sample stability), potential effects due to the operator, date of analysis, time of day collected, storage time before dry purging, sample storage time after dry purging, and collection volume were assessed and, where necessary, accounted for in the batch correction. In addition to the routine analysis of reference standards used to monitor retention shift and instrument response, the TD-GC×GC analytical system underwent a programmed heat cycle between each sample to reduce potential issues arising from sample carry-over, and a TD-trap blank and empty sorbent tube were analyzed every six samples to monitor the instrument baseline signal.

TDA in the discovery and replication sets

In TDA, the *x-y* coordinate position of a particular patient within a TDA cluster cannot be directly compared between discovery and

replication TDA graphs because the graphs represent a simple two-dimensional projection of a higher-dimensional structure. Before performing TDA, each feature was (x + 1) transformed. TDA parameters were set as number of hypercubes = 20, where the number of hypercubes refers to the number of overlapping intervals of the projection.

The distance between data points was measured using the Euclidean distance. The first two linear discriminant functions (LD1) and (LD2) were used as the projection. Clustering on the overlapping intervals on the projection was done using agglomerative (bottom up) hierarchical clustering with complete linkage. TDA was performed using Kepler Mapper 1.4.0 (*36*) with Python 3.5. Here, we computed the equivalence between topological data shapes generated using 805 volatile features extracted from the GC×GC-MS peak data, in both the discovery and replication cohorts.

Breath biomarker score generation

Feature selection was implemented via Lasso and elastic-net regularized generalized linear models (GLMNET) using the glmnet package in R. After removing features present in <80% of all samples from the (x + 1) transformed discovery GC×GC-MS peak data, a 735-feature matrix was obtained. A multinomial regression model using LASSO regularization was fitted to the 735-feature matrix in the discovery set using 10-fold cross-validation, with the dependent variable in the model being clinical diagnosis (acute asthma, acute COPD, pneumonia, heart failure, or healthy volunteers). The 10-fold cross-validation was repeated 100 times; features that had a nonzero regression coefficient in more than 80 of the cross-validation runs were considered as being stable candidate features predictive of the outcome (clinical diagnosis), and this resulted in 278 stable candidate features. For validation, predictors were calculated using the Predict function of GLMNET.

A multinomial regression model using elastic net regularization was fitted to the 278 features with the dependent variable in the model being clinical diagnosis. Following the chemometric inspection detailed above and the LASSO and elastic regression analysis, a final set of 101 exhaled breath volatile compounds was generated.

A multinomial regression model using elastic net regularization was fitted to the matrix of 101 breath biomarkers with the 10-fold cross-validation repeated 100 times. The R package glmnetUtils was used to determine the optimal value of α, the elastic net penalty; the best value for α was 0 (Ridge regression). Ridge regression with a logit link function (binary logistic regression) was fitted to the 101 breath relevant features; the dependent variable was "acute disease," as a binary outcome. The linear predictor from the combination of the most stable features was used as a score to predict acute disease. Linear combinations of the most stable features from the multinomial regression model fitted to the 101 biomarkers formed a set of scores for predicting probability of belonging to the different disease groups (acute asthma, acute COPD, pneumonia, heart failure, or healthy volunteers). Sensitivity analysis for the interactive elastic net regression approach and justification of the optimal α values are provided in figs. S11 to S12 and tables S6 to S8.

Figure S13 is a graphical probability distribution of the final 101 exhaled breath features in the GC×GC-MS peak data. The features largely follow a similar distribution. Some features contained a mixture of zero and nonzero values, which have arisen owing to the measurement being below the instrument's lower limit of detection. Constant features (all zero values) were removed before fitting the main model.

Breath biomarker coexpression and feature enrichment analysis

It was of interest to investigate if within the final set of 101 features, sets of "coexpressed" features existed, i.e., sets containing features that are correlated. Considering sets of coexpressed features has value in terms of reducing the dimensions of a problem and mitigating the multiple testing problem through the use of enrichment score. Coexpression and feature enrichment analysis are described in the Supplementary Materials section "Coexpression and feature enrichment analysis." Metabolite sets were derived on the basis of Ward hierarchical cluster analysis using the ChemRICH method reported in (*13*), and broader communities were derived from Louvain cluster analysis to help interpret the correlation graphs (Supplementary Materials section Coexpression and feature enrichment analysis). Covariation among metabolites lacks evidential value on its own; therefore, set-level significance was established using the Kolmogorov-Smirnov test (K-S test) as described using the ChemRICH method (*13*), Tanimoto coefficients were calculated to asses intraset chemical similarity using Metabox (*37*), and the frequency of occurrence in the published literature and relevant databases considered (KEGG, ChEBI, Human Metabolome Database, Human Breathomics Database, and microbial VOC database). Chemical similarity is of interest because compounds derived from similar pathways may also share common structural features or chemical groups. This combined data-driven and chemistry-driven approach has been shown to improve enrichment analysis (*13*, *38*) and allowed further interpretation of core findings here (fig. S10).

Statistical procedures

Statistical analysis was performed using R [3.6.1 and 4.0.0, R Core Team (2019)]. This research used the SPECTRE High-Performance Computing Facility at the University of Leicester. Baseline data and figures were presented as means ± SD and median (interquartile range). Data were analyzed using analysis of variance (ANOVA) to assess the differences between groups for normally or approximately normally distributed variables and Kruskal-Wallis for non-normally distributed variables. Pearson chi-square and Fisher's exact were used to assess the differences in categorical variables. All P values are two-sided and significant at the 0.05 level, unless reported otherwise.

Supplementary Materials

This PDF file includes:
Materials and Methods
Figs. S1 to S13
Tables S1 To S15

Other Supplementary Material for this manuscript includes the following:
Data file S1
MDAR Reproducibility Checklist

View/request a protocol for this paper from *Bio-protocol*.

REFERENCES AND NOTES

1. A. Hutchinson, A. Pickering, P. Williams, J. M. Bland, M. J. Johnson, Breathlessness and presentation to the emergency department: A survey and clinical record review. *BMC Pulm. Med.* **17**, 53 (2017).
2. M. B. Parshall, R. M. Schwartzstein, L. Adams, R. B. Banzett, H. L. Manning, J. Bourbeau, P. M. Calverley, A. G. Gift, A. Harver, S. C. Lareau, D. A. Mahler, P. M. Meek, D. E. O'Donnell; American Thoracic Society Committee on Dyspnea, An official American Thoracic Society statement: Update on the mechanisms, assessment, and management of dyspnea. *Am. J. Respir. Crit. Care Med.* **185**, 435–452 (2012).
3. W. Ibrahim, L. Carr, R. Cordell, M. J. Wilde, D. Salman, P. S. Monks, P. Thomas, C. E. Brightling, S. Siddiqui, N. J. Greening, Breathomics for the clinician: The use of volatile organic compounds in respiratory diseases. *Thorax* **76**, 514–521 (2021).
4. F. N. Schleich, D. Zanella, P. H. Stefanuto, K. Bessonov, A. Smolinska, J. W. Dallinga, M. Henket, V. Paulus, F. Guissard, S. Graff, C. Moermans, E. F. M. Wouters, K. Van Steen, F. J. van Schooten, J. F. Focant, R. Louis, Exhaled volatile organic compounds are able to discriminate between neutrophilic and eosinophilic asthma. *Am. J. Respir. Crit. Care Med.* **200**, 444–453 (2019).
5. M. J. Wilde, R. L. Cordell, D. Salman, B. Zhao, W. Ibrahim, L. Bryant, D. Ruszkiewicz, A. Singapuri, R. C. Free, E. A. Gaillard, C. Beardsmore, C. L. P. Thomas, C. E. Brightling, S. Siddiqui, P. S. Monks, Breath analysis by two-dimensional gas chromatography with dual flame ionisation and mass spectrometric detection - Method optimisation and integration within a large-scale clinical study. *J. Chromatogr. A* **1594**, 160–172 (2019).
6. K. A. Holden, W. Ibrahim, D. Salman, R. Cordell, T. McNally, B. Patel, R. Phillips, C. Beardsmore, M. Wilde, L. Bryant, A. Singapuri, P. Monks, C. Brightling, N. Greening, P. Thomas, S. Siddiqui, E. A. Gaillard, Use of the ReCIVA device in breath sampling of patients with acute breathlessness: A feasibility study. *ERJ Open Res.* **6**, 00119–02020 (2020).
7. P. Y. Lum, G. Singh, A. Lehman, T. Ishkanov, M. Vejdemo-Johansson, M. Alagappan, J. Carlsson, G. Carlsson, Extracting insights from the shape of complex data using topology. *Sci. Rep.* **3**, 1236 (2013).
8. J. L. Nielson, J. Paquette, A. W. Liu, C. F. Guandique, C. A. Tovar, T. Inoue, K.-A. Irvine, J. C. Gensel, J. Kloke, T. C. Petrossian, P. Y. Lum, G. E. Carlsson, G. T. Manley, W. Young, M. S. Beattie, J. C. Bresnahan, A. R. Ferguson, Topological data analysis for discovery in preclinical spinal cord injury and traumatic brain injury. *Nat. Commun.* **6**, –8581 (2015).
9. E. Somasundaram, A. Litzler, R. Wadhwa, S. Owen, J. Scott, Persistent homology of tumor CT scans is associated with survival in lung cancer. *Med. Phys.* **48**, 7043–7051 (2021).
10. S. Siddiqui, A. Shikotra, M. Richardson, E. Doran, D. Choy, A. Bell, C. D. Austin, J. Eastham-Anderson, B. Hargadon, J. R. Arron, A. Wardlaw, C. E. Brightling, L. G. Heaney, P. Bradding, Airway pathological heterogeneity in asthma: Visualization of disease microclusters using topological data analysis. *J. Allergy Clin. Immunol.* **142**, 1457–1468 (2018).
11. M. Nicolau, A. J. Levine, G. Carlsson, Topology based data analysis identifies a subgroup of breast cancers with a unique mutational profile and excellent survival. *Proc. Natl. Acad. Sci. U.S.A.* **108**, 7265–7270 (2011).
12. J. Brandsma, V. M. Goss, X. Yang, P. S. Bakke, M. Caruso, P. Chanez, S. E. Dahlén, S. J. Fowler, I. Horvath, N. Krug, P. Montuschi, M. Sanak, T. Sandström, D. E. Shaw, K. F. Chung, F. Singer, L. J. Fleming, A. R. Sousa, I. Pandis, A. T. Bansal, P. J. Sterk, R. Djukanović, A. D. Postle, Lipid phenotyping of lung epithelial lining fluid in healthy human volunteers. *Metabolomics* **14**, 123 (2018).
13. D. K. Barupal, O. Fiehn, Chemical similarity enrichment analysis (ChemRICH) as alternative to biochemical pathway mapping for metabolomic datasets. *Sci. Rep.* **7**, 14567 (2017).
14. M. J. Wilde, B. Zhao, R. L. Cordell, W. Ibrahim, A. Singapuri, N. J. Greening, C. E. Brightling, S. Siddiqui, P. S. Monks, R. C. Free, Automating and extending comprehensive two-dimensional gas chromatography data processing by interfacing open-source and commercial software. *Anal. Chem.* **92**, 13953–13960 (2020).
15. L. W. Sumner, A. Amberg, D. Barrett, M. H. Beale, R. Beger, C. A. Daykin, T. W. M. Fan, O. Fiehn, R. Goodacre, J. L. Griffin, T. Hankemeier, N. Hardy, J. Harnly, R. Higashi, J. Kopka, A. N. Lane, J. C. Lindon, P. Marriott, A. W. Nicholls, M. D. Reily, J. J. Thaden, M. R. Viant, Proposed minimum reporting standards for chemical analysis Chemical Analysis Working Group (CAWG) Metabolomics Standards Initiative (MSI). *Metabolomics* **3**, 211–221 (2007).
16. M. Basanta, B. Ibrahim, R. Dockry, D. Douce, M. Morris, D. Singh, A. Woodcock, S. J. Fowler, Exhaled volatile organic compounds for phenotyping chronic obstructive pulmonary disease: A cross-sectional study. *Respir. Res.* **13**, 72 (2012).
17. S. J. Fowler, M. Basanta-Sanchez, Y. Xu, R. Goodacre, P. M. Dark, Surveillance for lower airway pathogens in mechanically ventilated patients by metabolomic analysis of exhaled breath: A case-control study. *Thorax* **70**, 320–325 (2015).
18. A. Pizzini, W. Filipiak, J. Wille, C. Ager, H. Wiesenhofer, R. Kubinec, J. Blaško, C. Tschurtschenthaler, C. A. Mayhew, G. Weiss, R. Bellmann-Weiler, Analysis of volatile organic compounds in the breath of patients with stable or acute exacerbation of chronic obstructive pulmonary disease. *J. Breath Res.* **12**, 036002 (2018).
19. R. Peltrini, R. Cordell, W. Ibrahim, M. Wilde, D. Salman, A. Singapuri, B. Hargadon, C. E. Brightling, C. L. P. Thomas, P. Monks, S. Siddiqui, Volatile organic compounds in a headspace sampling system and asthmatics sputum samples. *J. Breath Res.* **15**, 027102 (2021).
20. D. Zanella, M. Henket, F. Schleich, T. Dejong, R. Louis, J.-F. Focant, P.-H. Stefanuto, Comparison of the effect of chemically and biologically induced inflammation on the volatile metabolite production of lung epithelial cells by GC×GC-TOFMS. *Analyst* **145**, 5148–5157 (2020).
21. R. Schnabel, R. Fijten, A. Smolinska, J. Dallinga, M.-L. Boumans, E. Stobberingh, A. Boots, P. Roekaerts, D. Bergmans, F. J. van Schooten, Analysis of volatile organic compounds in exhaled breath to diagnose ventilator-associated pneumonia. *Sci. Rep.* **5**, 17179 (2015).
22. J. Phan, S. Meinardi, B. Barletta, D. R. Blake, K. Whiteson, Stable isotope profiles reveal active production of VOCs from human-associated microbes. *J. Breath Res.* **11**, 017101 (2017).
23. D. Salman, M. Eddleston, K. Darnley, W. H. Nailon, D. B. McLaren, A. Hadjithelki, D. Ruszkiewicz, J. Langejuergen, Y. Alkhalifa, I. Phillips, C. L. P. Thomas, Breath markers for therapeutic radiation. *J. Breath Res.* **15**, 016004 (2021).
24. A. Sponring, W. Filipiak, T. Mikoviny, C. Ager, J. Schubert, W. Miekisch, A. Amann, J. Troppmair, Release of volatile organic compounds from the lung cancer cell line NCI-H2087 in vitro. *Anticancer Res.* **29**, 419–426 (2009).
25. W. Filipiak, A. Sponring, A. Filipiak, C. Ager, J. Schubert, W. Miekisch, A. Amann, J. Troppmair, TD-GC-MS analysis of volatile metabolites of human lung cancer and normal Cells In vitro. *Cancer Epidemiol. Biomarkers Prev.* **19**, 182–195 (2010).
26. A. Sponring, W. Filipiak, C. Ager, J. Schubert, W. Miekisch, A. Amann, J. Troppmair, Analysis of volatile organic compounds (VOCs) in the headspace of NCI-H1666 lung cancer cells. *Cancer Biomark.* **7**, 153–161 (2010).
27. M. Koureas, P. Kirgou, G. Amoutzias, C. Hadjichristodoulou, K. Gourgoulianis, A. Tsakalof, Target analysis of volatile organic compounds in exhaled breath for lung cancer discrimination from other pulmonary diseases and healthy persons. *Metabolites* **10**, 317 (2020).
28. M. K. David Ponka, Top differential diagnoses in family medicine Dyspnoea can Fam physician. Canadian Family Physician, (2008).
29. S. Laribi, G. Keijzers, O. van Meer, S. Klim, J. Motiejunaite, W. S. Kuan, R. Body, P. Jones, M. Karamercan, S. Craig, V.-P. Harjola, A. Holdgate, A. Golea, C. Graham, F. Verschuren, J. Capsec, M. Christ, L. Grammatico-Guillon, C. Barletta, L. Garcia-Castrillo, A.-M. Kelly; AANZDEM and EURODEM study groups, Epidemiology of patients presenting with dyspnea to emergency departments in Europe and the Asia-Pacific region. *Eur. J. Emerg. Med.* **26**, 345–349 (2019).
30. W. Ibrahim, M. Wilde, R. Cordell, D. Salman, D. Ruszkiewicz, L. Bryant, M. Richardson, R. C. Free, B. Zhao, A. Yousuf, C. White, R. Russell, S. Jones, B. Patel, A. Awal, R. Phillips, G. Fowkes, T. McNally, C. Foxon, H. Bhatt, R. Peltrini, A. Singapuri, B. Hargadon, T. Suzuki, L. L. Ng, E. Gaillard, C. Beardsmore, K. Ryanna, H. Pandya, T. Coates, P. S. Monks, N. Greening, C. E. Brightling, P. Thomas, S. Siddiqui, Assessment of breath volatile organic compounds in acute cardiorespiratory breathlessness: A protocol describing a prospective real-world observational study. *BMJ open* **9**, e025486 (2019).
31. P. M. Bossuyt, J. B. Reitsma, D. E. Bruns, C. A. Gatsonis, P. P. Glasziou, L. Irwig, J. G. Lijmer, D. Moher, D. Rennie, H. C. de Vet, H. Y. Kressel, N. Rifai, R. M. Golub, D. G. Altman, L. Hooft, D. A. Korevaar, J. F. Cohen; STARD Group, STARD 2015: An updated list of essential items for reporting diagnostic accuracy studies. *BMJ* **351**, h5527 (2015).
32. G. S. Collins, J. B. Reitsma, D. G. Altman, K. G. Moons, Transparent reporting of a multivariable prediction model for individual Prognosis Or Diagnosis (TRIPOD): The TRIPOD statement. *Br. J. Surg.* **102**, 148–158 (2015).
33. K. G. M. Moons, D. G. Altman, J. B. Reitsma, J. P. A. Ioannidis, P. Macaskill, E. W. Steyerberg, A. J. Vickers, D. F. Ransohoff, G. S. Collins, Transparent reporting of a multivariable prediction model for Individual Prognosis Or Diagnosis (TRIPOD): Explanation and elaboration. *Ann. Intern. Med.* **162**, W1–W73 (2015).
34. S. Kitchen, A. Edge, R. Smith, P. Thomas, S. Fowler, S. Siddiqui, M. van der Schee, LATE-BREAKING ABSTRACT: Breathe free: Open source development of a breath sampler by a consortium of breath researchers. *Eur. Respir. J.* **46**, (2015).
35. B. Zhao, L. Bryant, R. Cordell, M. Wilde, D. Salman, D. Ruszkiewicz, W. Ibrahim, A. Singapuri, T. Coats, E. Gaillard, C. Beardsmore, T. Suzuki, L. Ng, N. Greening, P. Thomas, P. Monks, C. Brightling, S. Siddiqui, R. C. Free, LabPipe: An extensible bioinformatics toolkit to manage experimental data and metadata. *BMC Bioinformatics* **21**, 556 (2020).
36. H. J. van Veen, N. Saul, D. Eargle, S. W. Mangham, Kepler Mapper: A flexible Python implementation of the Mapper algorithm. *Zenodo*, (2021).
37. K. Wanichthanarak, S. Fan, D. Grapov, D. K. Barupal, O. Fiehn, Metabox: A toolbox for metabolomic data analysis, interpretation and integrative exploration. *PLOS ONE* **12**, e0171046 (2017).
38. J. R. Ash, M. A. Kuenemann, D. Rotroff, A. Motsinger-Reif, D. Fourches, Cheminformatics approach to exploring and modeling trait-associated metabolite profiles. *J. Chem.* **11**, 43 (2019).

Acknowledgments: The work was carried out at the University Hospitals of Leicester NHS Trust, University of Leicester and Loughborough University, supported by the NIHR Leicester Biomedical Research Center and the NIHR Leicester Clinical Research Facility. We would like to thank the wider East Midlands Breathomics Pathology Node Consortium. **Funding:** This research was funded by the Medical Research Council (MRC), Engineering and Physical Sciences Research Council (EPSRC) Stratified Medicine Grant for Molecular Pathology Nodes (grant no. MR/N005880/1), Midlands Asthma and Allergy Research Association (MAARA), and British Lung Foundation (grant no. BLFPHD17-1). The research was supported by the National Institute for Health Research (NIHR) Leicester Biomedical Research Center and NIHR, Leicester Clinical Research Facility, the Leicester Wellcome Trust ISSF (award no. 204801/Z/16/Z), and the MAARA to whom we are grateful. N.J.G. is funded by an NIHR postdoctoral fellowship (PDF-2017-10-052). The views expressed are those of the author(s) and not necessarily those of the NHS, the NIHR, or the Department of Health and Social Care. **Author contributions:** S.S., C.E.B., N.J.G., P.T., and P.S.M. conceived the study, obtained funding, wrote the study protocol, obtained ethical and MHRA approvals for the study, and coordinated the deployment of analytical testing methods for breath analysis. W.I. has led planning and recruitment of study participants as well as taking the lead in writing the manuscript, with support from S.S., R.L.C., N.J.G., M.J.W., and M.R. Analytical chemistry team formed of M.J.W and R.L.C led the analytical method development, the development of all breath sampling and analytical protocols, pre- and postclinic preparation and analysis of breath samples, and data processing of chemical and analytical data. M.R., a senior statistician, constructed a statistics and data analysis plan in conjunction with S.S. and M.J.W. Bioinformatics pipeline and electronic CRFs were developed by R.C.F. and B.Z. All authors, including D.S., A.S., B.H., E.A.G., T.S., L.L.N., and T.C., contributed to the study design. All authors contributed to and approved the manuscript. **Competing interests:** C.E.B. has received consultancy and/or grants paid to his institution from GlaxoSmithKline (GSK), Astrazeneca (AZ), Boehringer Ingelheim (BI), Novartis, Chiesi, Genentech, Roche, Sanofi, Regeneron, TEVA Pharmaceuticals, MSD, Mologic, CSL Behring, Gossamer, and 4Dpharma. S.S. has received funding from the MRC/EPSRC and University of Leicester for the research program presented in the manuscript. S.S. has engaged in consultancies/received speaker fees related to asthma, COPD, lung physiology, and eosinophilic airway diseases from the following companies: Boehringer Ingelheim, Chiesi, Novartis, GSK, AZ, ERT Medical, Owlstone Medical, CSL Behring, Mundipharma, and Knopp biotech. E.G. reports consultancy work for Boehringer Ingelheim with money paid to the institution (University of Leicester); investigator-led research grant from Circassia Group, Gilead Sciences, Chiesi Limited, and Propeller Health; research collaboration with Medimmune and Adherium (NZ) Limited; and speaker fees from Circassia Group. The work presented in this paper has been filed by S.S., R.C., M.W., C.E.B., D.S., and P.T. as part of the U.K. Patent application no. 2110365.0 and International Patent application no. PCT/GB2022/051858. The rest of the coauthors declare that they have no competing interests. **Data and materials availability:** All data associated with this study are available in the main text or the Supplementary Materials. R and Python codes have been archived in Zenodo (https://doi.org/10.5281/zenodo.6956451). Access to anonymized core patient-level data used to generate results in this manuscript are available via request from senior author (S.S.; email: s.siddiqui@imperial.ac.uk) and are subject to MRC EMBER steering group approval and fully executed material transfer agreement with the University of Leicester as the study sponsor.

The EMBER Consortium: In addition to EMBER Consortium members who are authors (W.I., M.J.W., R.L.C., M.R., D.S., R.C.F., B.Z., A.S., B.H., E.A.G., T.S., L.L.N., T.C., P.T., P.S.M., C.E.B., N.J.G., and S.S.), the following EMBER Consortium members are collaborators who have contributed to the study design, data analysis, and interpretation: Rachel Munton[11], John Le Quesne[12], Alison H. Goodall[1], Hitesh C. Pandya[1,13], James C. Reynolds[4], Martha R. J. Clokie[1], Nilesh J. Samani[1], Michael R. Barer[1], and Jacqueline A. Shaw[1]. Affiliations 1 to 10 can be found on the first page of the paper. [11]East Midlands Academic health Science Network, University of Nottingham Innovation Park, Nottingham NG7 2TU, UK. [12]University of Glasgow, Glasgow S12 8QQ, UK. [13]AstraZeneca PLC, 2 Kingdom Street, London W2 6BD, UK.

Submitted 27 July 2021
Resubmitted 24 May 2022
Accepted 18 October 2022
Published 16 November 2022
10.1126/scitranslmed.abl5849

Science Translational Medicine

Visualization of exhaled breath metabolites reveals distinct diagnostic signatures for acute cardiorespiratory breathlessness

Wadah IbrahimMichael J. WildeRebecca L. CordellMatthew RichardsonDahlia SalmanRobert C. FreeBo ZhaoAmisha SingapuriBeverley HargadonErol A. GaillardToru SuzukiLeong L. NgTim CoatsPaul ThomasPaul S. MonksChristopher E. BrightlingNeil J. GreeningSalman Siddiqui, and Rachel Munton, and John Le Quesne, and Alison H. Goodall, and Hitesh C. Pandya, and James C. Reynolds, and Martha R. J. Clokie, and Nilesh J. Samani, and Michael R. Barer, and Jacqueline A. Shaw

Sci. Transl. Med., 14 (671), eabl5849. • DOI: 10.1126/scitranslmed.abl5849

Take my breath(lessness) away

Breath analysis can be a useful noninvasive way to detect disease. Here, Ibrahim *et al.* studied the volatile organic compound (VOC) signatures associated with acute cardiorespiratory diseases in patients presenting breathlessness. Using two-dimensional gas chromatography and mass spectrometry, the authors found clusters of VOCs associated with acute heart failure, asthma, chronic obstructive pulmonary disease, and pneumonia. These breath biomarkers correlated with blood-based biomarkers. An acute disease VOC score based on a 101-biomarker panel was associated with 2-year all-cause mortality. This study demonstrates how breathomics can help diagnose disease and further our understanding of metabolic subgroups.

Science Translational Medicine (ISSN) is published by the American Association for the Advancement of Science. 1200 New York Avenue NW, Washington, DC 20005. The title *Science Translational Medicine* is a registered trademark of AAAS.